

ARLCB

TR-85005

AD

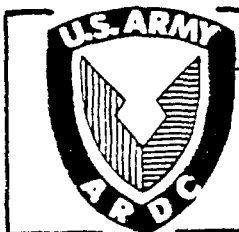
TECHNICAL REPORT ARLCB-TR-85005

**THERMAL EXPANSION EFFECTS IN ELECTRICAL
TRANSPORT IN AMORPHOUS METALS**

L. V. MEISEL

P.J. COTE

FEBRUARY 1985



**US ARMY ARMAMENT RESEARCH AND DEVELOPMENT CENTER
LARGE CALIBER WEAPON SYSTEMS LABORATORY
BENET WEAPONS LABORATORY
WATERVLIET N.Y. 12189**

DISCLAIMER

The findings in this report are not to be construed as an official Department of the Army position unless so designated by other authorized documents.

The use of trade name(s) and/or manufacture(s) does not constitute an official indorsement or approval.

DISPOSITION

Destroy this report when it is no longer needed. Do not return it to the originator.

REPORT DOCUMENTATION PAGE		READ INSTRUCTIONS BEFORE COMPLETING FORM
1. REPORT NUMBER ARLCB-TR-85005	2. GOVT ACCESSION NO.	3. RECIPIENT'S CATALOG NUMBER
4. TITLE (and Subtitle) THERMAL-EXPANSION EFFECTS IN ELECTRICAL TRANSPORT IN AMORPHOUS METALS		5. TYPE OF REPORT & PERIOD COVERED Final
		6. PERFORMING ORG. REPORT NUMBER
7. AUTHOR(s) L. V. Meisel and P. J. Cote		8. CONTRACT OR GRANT NUMBER(s)
9. PERFORMING ORGANIZATION NAME AND ADDRESS US Army Armament Research & Development Center Benet Weapons Laboratory, SMCAR-LCB-TL Watervliet, NY 12189-5000		10. PROGRAM ELEMENT, PROJECT, TASK AREA & WORK UNIT NUMBERS AMCMS No. 6111.02.H600.011 PRON No. 1A325B541A1A
11. CONTROLLING OFFICE NAME AND ADDRESS US Army Armament Research & Development Center Large Caliber Weapon Systems Laboratory Dover, NJ 07801-5001		12. REPORT DATE February 1985
		13. NUMBER OF PAGES 26
14. MONITORING AGENCY NAME & ADDRESS (if different from Controlling Office)		15. SECURITY CLASS. (of this report) Unclassified
		15a. DECLASSIFICATION/DOWNGRADING SCHEDULE
16. DISTRIBUTION STATEMENT (of this Report) Approved for public release; distribution unlimited		
17. DISTRIBUTION STATEMENT (of the abstract entered in Block 20, if different from Report)		
18. SUPPLEMENTARY NOTES To be published in Physical Review B Journal.		
19. KEY WORDS (Continue on reverse side if necessary and identify by block number) Disordered Metals Thermal Expansion Electrical Transport		
20. ABSTRACT (Continue on reverse side if necessary and identify by block number) Theoretical treatments of electrical transport in amorphous metals are usually performed at constant volume, although most experimental studies are performed at constant pressure. Recent studies of the influence of pressure on the electrical resistivity of a variety of amorphous metals indicate that thermal expansion effects can not be ignored in a theoretical description of the temperature dependence of the isobaric resistivity. In this report, general (CONT'D ON REVERSE)		

20. ABSTRACT (CONT'D)

ideas pertinent to a theoretical description of non-isochoric electrical transport are presented. Results for isobaric electrical transport based on the Gruneisen theory of thermal expansion, which are independent of the model employed to treat isochoric transport, are also given. The implications of the theory are illustrated in the context of the diffraction model by: (1) detailed results specific to the well-characterized low resistivity alloy, α -Mg₇Zn₃; and (2) a selection of model calculations incorporating thermal expansion effects for cases with positive and negative pressure coefficients of resistivity.

TABLE OF CONTENTS

	<u>Page</u>
INTRODUCTION	1
THEORY	2
RESULTS	6
CONCLUSIONS	14
REFERENCES	18

TABLES

I. PARAMETERS EMPLOYED IN THE a-Mg ₇ Zn ₃ CALCULATIONS.	20
---	----

LIST OF ILLUSTRATIONS

1. The Debye integral, defined in Eq. (4b), and its first derivative.	21
2. The relative change in resistivity versus temperature for a-Mg ₇ Zn ₃ based on the parameters in Table I. Curves A, B, and C are computed for $q_D\Lambda = \infty$ (the standard diffraction model); curves D, E, F for $q_D\Lambda = 17.1$. Curves A and D are isochoric results. Curves B and E include thermal expansion effects with the measured ⁴ pressure coefficient of resistivity Π . Curves C and F include thermal expansion effects with Hafner's ⁵ theoretical Π . Dashed curve shows experimental data from Reference 7; arrow indicates breadth of scatter band.	22
3. Normalized resistivity difference versus normalized temperature for potassium pseudoatom phase shifts ¹⁹ with $2k_F/k_p = 1.1$ and $q_D\Lambda = 12$. The w values are 0.5, 0.2, 0, -0.2, and -0.5 for curves A, B, C, D, and E, respectively.	23
4. Same as Figure 3 for the constant t-matrix effective potential approximation ¹⁶ with $2k_F/k_p = 1.15$ and $q_D\Lambda = 12$.	24
5. Same as Figure 3 for the constant t-matrix effective potential approximation ¹⁶ with $2k_F/k_p = 1.30$ and $q_D\Lambda = 6$.	25

INTRODUCTION

Experimental determinations of the temperature T dependence of the electrical resistivity ρ in amorphous metals have generally been made at constant pressure P . Nevertheless, most theoretical studies of electrical transport in amorphous metals have treated the variation of ρ with T at constant volume V . This has been the case because: (1) there were few published measurements of $\rho(T)$ at pressure; (2) the available data did not seem to show any regularity; and (3) the early experimental studies (refs 1,2) which were performed in high ρ , TM-based, amorphous alloys, exhibited pressure coefficients of resistivity that were considerably smaller in magnitude than those in lower ρ , crystalline alloys (ref 3).

However, recent experimental studies of the effects of pressure on electrical transport in amorphous metals by Fritsch, Willer, Wildermuth, and Luscher (ref 4) indicate that thermal expansion effects cannot generally be ignored. Recently, Hafner (ref 5) found that thermal expansion effects are important in determining the T -dependence of ρ at constant pressure in α -Mg₇Zn₃ in a pseudopotential based, diffraction model calculation. Furthermore, reexamination of the early data, assuming reasonable values for the bulk moduli B_T , suggests that thermal expansion effects can also be important in high resistivity alloys.

Thus, it is our objective to give a simple description of the way that thermal expansion effects influence the $\rho(T)$ in amorphous metals. Although we present examples in the context of the diffraction model, our principal results are not transport model specific. Our approach is to assume that

References are listed at the end of this report.

macroscopic properties such as $B_T(T)$, the Gruneisen constant $\gamma(T)$, $\partial \ln \rho / \partial \ln V|_T$, etc., are given and that the thermal expansion (i.e., $V(T)$) is described by Gruneisen's law (ref 6). This approach is in contrast to the tour de force of Hafner (ref 5), in which all relevant quantities are computed from first principles using pseudopotential methods specifically for a-Mg₇Zn₃ and a-Ca₇Mg₃.

THEORY

The variations of ρ with volume variations produced by thermal expansion are small compared to ρ for $0 < T < 2\theta$ in amorphous metals. Thus, one may expand ρ in a Taylor series in $\ln(V)$ and neglect terms higher than first order:

$$\rho(T, V) = \rho(T, V_0) [1 + Q(T, V)] \quad (1a)$$

where the thermal expansion part,

$$Q(T, V) \equiv \ln(V/V_0) \frac{\partial \ln \rho}{\partial \ln V} \Big|_{T, V_0} \quad (1b)$$

and V_0 is the mean atomic volume at 0°K and one atmosphere. Similarly, the isochoric variations in ρ are small compared to ρ for $0 < T < 2\theta$ so that we may rewrite Eq. (1) as

$$\rho(T, V) = \rho_0 [1 + R(T, V_0) + Q(T, V)] \quad (2)$$

where $\rho_0 \equiv \rho(0, V_0)$ and $R(T, V_0)$ is the isochoric relative change in resistivity, i.e.,

$$R(T, V_0) \equiv \rho(T, V_0) / \rho_0 - 1 \quad (2a)$$

Note that we drop the higher order $R(T, V_0) Q(T, V)$ term to obtain Eq. (2).

Now, $\ln(V(T)/V_0) \approx V(T)/V_0 - 1$ since $V(T)/V_0 - 1 \ll 1$ for $0 < T < 2\theta$.

Thus, Gruneisen's law (ref 6) of thermal expansion yields at constant pressure:

$$\ln(V/V_0) = \overline{\gamma \epsilon(T)} / B_T V_0 \quad (3)$$

where $\overline{\epsilon(T)}$ is the mean thermal energy, γ is the Gruneisen constant, and B_T is the bulk modulus. The mean thermal energy can then be evaluated for a Debye model, yielding

$$\overline{\epsilon(T)} = 3Nk_B \theta F(T/\theta) \quad (4a)$$

where N is the avagadro's number, k_B is the Boltzmann constant, and

$$F(x) \equiv x^4 \int_0^{1/x} 3z^3 dz / (e^z - 1) \quad (4b)$$

The limiting forms of $F(T/\theta)$ are

$$F(T/\theta) = (\pi^4/5)(T/\theta)^4 \quad \text{for } T/\theta \ll 1 \quad (4c)$$

and

$$F(T/\theta) = T/\theta \quad \text{for } T/\theta \gg 1 \quad (4d)$$

Figure 1 exhibits graphs of $F(T/\theta)$ and $F'(T/\theta)$ versus T/θ . $F(T/\theta)$ and $F'(T/\theta)$ describe the T -dependence of $\overline{\epsilon(T)}$ and the lattice specific heat $C_V(T)$, respectively, in the Debye model. We shall see below that the thermal expansion part of the isobaric $\rho(T)$ is proportional to $F(T/\theta)$ and that the thermal expansion coefficient is proportional to $F'(T/\theta)$.

Thus, our principal result at constant pressure is

$$\rho(T) = \rho(T, V(T))|_p = \rho_0(1 + R(T, V_0) + Q(T)) \quad (5)$$

where

$$Q(T) \equiv Q(T, V(T))|_p = K(T)F(T/\theta) \quad (6a)$$

$$\text{with } K(T) \equiv (3Nk_B \theta(T) \gamma(T) / B_T(T) V_0) (\partial \ln \rho / \partial \ln V)_{T, V_0} \quad (6b)$$

and $R(T, V_0)$ is the isochoric relative change in ρ defined in Eq. (2a). The T -dependence of $K(T)$ is much weaker than that of $F(T/\theta)$. Moreover, at low T ,

where the temperature variation of $K(T)$ is largest, $F(T/\theta)$ varies very rapidly with T (i.e., like T^4) and is small. Thus, it is a good approximation to neglect the T variation of $K(T)$ and to use $K(T) \approx K(\theta)$.

An alternate expression for $K(\theta)$ can be derived in terms of the thermal expansion coefficient $\beta_V(T)$,

$$\beta_V(T) \equiv (\partial \ln V / \partial T)_P \approx 3Nk_B \gamma(T) F'(T/\theta) / B_T(T) V_0 \quad (7)$$

where we have neglected the $\overline{\epsilon(T)} \partial(\gamma/B_T V_0) / \partial T$ term and a term arising from $\partial \theta / \partial T$. (Equation (7) is equivalent to Eq. (9) of Reference 5.) Then substituting Eq. (7) in Eq. (6b) at $T = \theta$, one finds

$$\begin{aligned} K(\theta) &= \beta_V(\theta) \theta(\theta) (\partial \ln \rho / \partial \ln V)_{\theta, V_0} / F'(1) \\ &\approx 1.05 \theta \beta_V(\theta) (\partial \ln \rho / \partial \ln V)_{\theta, V_0} \end{aligned} \quad (8)$$

(Equivalent expressions can be given if $\beta_V(T)$ is known at some other T .)

Equations (5), (6a), and (8) thus also serve as a basis for the discussion of thermal expansion effects in electrical transport. Clearly, if $K(T)$ is known one can use Eqs. (5) and (6) without further approximation to describe the thermal expansion part of $\rho(T)$.

Frequently, the pressure coefficient of resistance Π is experimentally accessible rather than $\partial \ln \rho / \partial \ln V|_{T, V_0}$. One then employs

$$\begin{aligned} \Pi(T) &\equiv (\partial \ln R / \partial P)_{T, V_0} = (\partial \ln R / \partial \ln V)_{T, V_0} (\partial \ln V / \partial P)_{T, V_0} \\ &= - (\partial \ln R / \partial \ln V)_{T, V_0} / B_T(T) \end{aligned} \quad (9a)$$

$$= - ((\partial \ln \rho / \partial \ln V)_{T, V_0} - 1/3) / B_T(T) \quad (9b)$$

or

$$\left(\frac{\partial \ln \rho}{\partial \ln V}\right)_{T, V_0} = - B_T(T) \Pi(T) + 1/3 \quad (9c)$$

where R is the resistance.

We will refer to isochoric and thermal expansion parts of the isobaric temperature coefficients of resistivity defined as

$$\Gamma \equiv \left. \frac{\partial \ln \rho}{\partial T} \right|_{T=\theta, P} \equiv \Gamma_{V_0} + \Gamma_{\beta} \quad (10a)$$

where the isochoric part is given by

$$\Gamma_{V_0} \equiv (\partial R(T, V_0) / \partial T)_{T=\theta} \quad (10b)$$

and the thermal expansion part is given by

$$\Gamma_{\beta} \equiv (\partial Q(T) / \partial T)_{T=\theta} \quad (10c)$$

$$= \beta_V(\theta) \left(\frac{\partial \ln \rho}{\partial \ln V}\right)_{\theta, V_0} \quad (10d)$$

$$= - \beta_V(\theta) (B_T(\theta) \Pi(\theta) - 1/3) \quad (10e)$$

Note that the description of thermal expansion effects on electrical transport presented here is model independent. That is, no matter which technique is used to compute the isochoric relative change in ρ (i.e., $R(T, V_0)$ in Eq. (15)), a thermal expansion correction $Q(T)$ is required to obtain the isobaric $\rho(T)$. The thermal expansion term will be observable in $\rho(T)$ whenever Π (or $\partial \ln \rho / \partial \ln V$) is sufficiently large in magnitude. Equation (6) with $F(x)$ defined in Eq. (4b) obtains if $V(T)$ is represented in terms of the Gruneisen theory of thermal expansion. Generally, $K(T)$, defined in Eq. (6b), is a weak function of T in comparison to $F(T/\theta)$ so that in the examples given here we treat $K(T)$ as a constant. Clearly, the T -dependence of $K(T)$ or a more general

theory for $V(T)$ and/or $(\partial \ln \rho / \partial \ln V)_{T, V_0}$ can be incorporated into the formalism, in a straightforward manner.

RESULTS

The thermal expansion part of the isobaric $\rho(T)$ is negligible in comparison to the isochoric part of the isobaric $\rho(T)$ at very low temperatures ($T < \theta/15$). One can see this effect in Figures 2 through 5. This is the case because $F(T/\theta)$ vanishes as $(T/\theta)^4$ while $R(T, V_0)$ vanishes approximately as $(T/\theta)^2$ at very low temperatures. The thermal expansion term is approximately linear in T above the Debye temperature and yields a "correction" to the isochoric temperature coefficient of resistivity Γ_{V_0} whose sign is determined by the sign of $(\partial \ln \rho / \partial \ln V)_{T, V_0}$.

The best characterized and most thoroughly studied low resistivity ($\sim 60 \mu\Omega\text{cm}$) amorphous alloy is a-Mg₇Zn₃ (refs 4,7). It is the only low resistivity alloy for which the pressure coefficient of resistance Π has been determined. The isobaric $\rho(T)$ has the following features: (1) a small minimum at $T_m \approx 7\text{K}$; (2) a maximum at $T_M \approx 40\text{K}$; (3) an approximately $(T-T_M)^{3/2}$ region for $T > T_M$; and (4) approximately linear T -dependence near 300K with $\Gamma \approx -2.0 \times 10^{-4}/\text{K}$. The low temperature results from Reference 7 are shown in Figure 2.

Since a-Mg₇Zn₃ is the only low resistivity alloy with known Π (ref 4), we will provide a somewhat extended description of the status of the theoretical work on this alloy and the importance of thermal expansion in determining $\rho(T)$. All the calculations have been performed in the context of Baym-Faber-Ziman theory (refs 8,9) (the diffraction model).

Hafner (ref 5) computed $\rho(T)$ in α -Mg₇Zn₃ from first principles in a pseudopotential based procedure with no saturation corrections. The volume dependence of ρ , Π , the isobaric T-dependence of ρ , the dynamical structure factor, and the pseudopotentials were all computed with no adjustable or empirical parameters. The agreement with the data is remarkable. Hafner concluded that thermal expansion effects are important in determining $\rho(T)$ in (liquid and) amorphous Mg₇Zn₃.

Meisel and Cote (ref 10) described isochoric diffraction model studies of $\rho(T)$ in the α -MgZn alloys (and low resistivity alloys in general). An effective scattering matrix was constructed which had exclusively s and p character, satisfied the Friedel sum rule, and yielded the observed magnitude of ρ . "Good" quantitative agreement with isobaric data was obtained when Pippard-Ziman saturation (refs 9,11-15) was included: (1) the computed Γ values were approximately half the observed values; (2) the temperatures T_M for the resistivity maxima were overestimated by approximately 30 percent; (3) the sizes of the maxima ($\rho(T_M)/\rho(0)-1$) were overestimated by a factor of two; (4) the temperatures T_m for the resistivity minima were overestimated by approximately 30 percent; and (5) the depths of the minima were underestimated by at least a factor of two. (These results are closely approximated by curve D of Figure 2.) When saturation effects were not included (i.e., when standard Baym-Faber-Ziman theory (ref 8) was applied) qualitative agreement with the data was still obtained (except for the minimum in ρ), although quantitative agreement with the data was severely diminished. (These results are closely approximated by curve A of Figure 2.)

A later discussion of isochoric diffraction model transport in a-MgZn by Cote and Meisel (ref 14) based upon phase shifts computed for Herman-Skillman (ref 15) neutral atom wavefunctions, suggested that the isobaric $\rho(T)$ could be fit if the Debye temperature for resistivity was taken as 200K instead of the thermal value of 295K. (The magnitude of ρ computed for these phase shifts is $40 \mu\Omega\text{cm}$, approximately 30 percent less than the measured value.) If θ is taken as 295K, the results of these calculations, shown in curve D of Figure 2, are not significantly different from those of the "effective potential" calculations described above.

Figure 2 shows results of diffraction model calculations based upon the phase shifts employed in Reference 14. Essentially the same results are obtained in constant t-matrix calculations as described in Reference 16 or effective potential calculations as described in Reference 10. The parameters used in the calculations are listed in Table I. Isochoric results are shown in curves A and D. Isobaric results computed using the pressure coefficient of resistivity Π value deduced from the experimental data of Fritsch et al (ref 4) are shown in curves B and E and results computed using the Π value computed by Hafner (ref 5) are shown in curves C and F. The isochoric part of ρ in curves A, B, and C is the standard Baym-Faber-Ziman (ref 8) results, while that in curves D, E, and F include Pippard-Ziman saturation (refs 9, 11-13) with $q_D\Lambda = 17.1$ where q_D is the Debye wave number and Λ the electron mean free path. The value of $q_D\Lambda$ was computed in the free electron approximation (Eq. (24) of Reference 16). That is,

$$q_D\Lambda = 644(Z/2)^{1/3} (k_{FH})^{-1} (\rho/\mu\Omega\text{cm})^{-1} \quad (11)$$

where Z is the electron per atom ratio and a_H the Bohr radius. Although Figure 2 displays results for $0 < T < 105K$, our discussion pertains to results for $0 < T < 300K$. That is, when we refer to curve F we mean the computed result for the specified parameter values for $0 < T < 300K$.

Curve F (incorporating Π computed by Hafner (ref 5) and $q_D \Lambda = 17.1$) agrees with the data quite well: (1) Temperature coefficient of resistivity Γ is given within 10 percent; (2) the position of the maximum $\rho(T)$, T_M is given within 10 percent; (3) the position of the minimum of $\rho(T)$, T_m is given within 10 percent; (4) the size of the maximum is underestimated by about 30 percent; and (5) the size of the minimum is significantly underestimated.

Curve E (incorporating Π deduced from the data of Fritsch et al (ref 4) and $q_D \Lambda = 17.1$) represents almost as good a fit to the data as curve F: (1) Γ is underestimated by about 25 percent; (2) T_M is overestimated by approximately 25 percent; (3) T_m is given within 10 percent; (4) the size of the maximum is given within 10 percent; and (5) the size of the minimum is significantly underestimated.

The curves of Figure 2 illustrate the action of thermal expansion effects for positive Π . They also illustrate the action of Pippard-Ziman saturation (refs 9,11-13) for a low resistivity ($q_D \Lambda \approx 17$) amorphous metal. Both effects yield more negative Γ , shift T_M to lower values, and reduce the size of the maximum of $\rho(T)$. However, at very low T , thermal expansion effects become negligible while saturation effects are still important (producing minima in $\rho(T)$, for example). (Note that Hafner's (ref 5) transport calculation, which does not include saturation, produces a minimum in $\rho(T)$. The origin of the calculated minimum is not clear. These calculations also underestimate the

size of the minimum.) It is evident that thermal expansion effects are important in determining $\rho(T)$ in a-Mg₇Zn₃ and are of the same order as saturation effects for this alloy.

When thermal expansion effects are included in diffraction model calculations based on Heine-Aberenkov pseudopotentials for Mg and Zn tabulated in Harrison (ref 18), qualitative agreement with the data is greatly improved, but quantitative results are still poor. (However, recall that Hafner's (ref 5) pseudopotential calculation agrees quite well with the data for a-Mg₇Zn₃.)

Figures 3 through 5 are examples of the effects of thermal expansion in determining isobaric ρ vs. T curves in the context of the diffraction model including the Pippard-Ziman saturation. The parameters and variables used in the figures are defined as follows:

$$\alpha \equiv 12\pi^2 k_F^2 / M k_B \theta \quad (12)$$

where M is the averaged ionic mass and k_F is the Fermi wavenumber. The parameter α determines the scale of the isochoric variations of ρ for given values of $2k_F/k_p$, $qD\Lambda$, etc.

For practical values of α , $R(T, V_0)/\alpha$ is approximately independent of α . Thus, we define the normalized relative change of the resistivity as

$$r \equiv (\rho(T)/\rho_0 - 1)/\alpha = R(T, V_0)/\alpha + Q(T)/\alpha \quad (13a)$$

$$\equiv R(T, V_0)/\alpha + w(T)F(T/\theta) \quad (13b)$$

where, in the approximation scheme which treats $K(T)$ as constant,

$$w(T) \approx w \equiv w(\theta) = -1.05 \theta \beta_V(\theta) \Pi / \alpha \quad (13c)$$

The thermal expansion part of Γ can then be expressed as

$$\Gamma_\beta = 0.95 \alpha w(\theta) / \theta \quad (13d)$$

We also define a normalized temperature,

$$t \equiv T/\theta \quad (13e)$$

Thus, Figures 3 through 5 are plots of normalized relative change of the resistivity r versus normalized temperature t for specific values of $2k_F/k_p$ and $q_D\Lambda$ and a range of values for the parameter w . The w values (viz., 0, ± 0.2 , and ± 0.5) were chosen to be representative of the range to be found in amorphous metals. The curves can be linearly interpolated or extrapolated to obtain results for other w values or to allow for a T -dependent $w(T)$. For example, in $a\text{-Mg}_7\text{Zn}_3$, $w \approx 0.16$ for the experimental⁴ Π and 0.33 for the theoretical (ref 5) Π .

Results based upon potassium pseudoatom phase shifts computed by Young, Meyer, and Kilby (ref 19) for $2k_F/k_p = 1.1$ and $q_D\Lambda = 12$ are shown in Figure 3. The pseudoatom phase shift absolute squared t -matrices are very similar to absolute squared pseudopotential matrix elements except that they do not exhibit perfect cancellation near $2k_F$. Thus, Figure 3 is very similar to a pseudopotential result. Isochoric $\rho(T, V_0)$ has a maximum near $\theta/2$ and Γ_{V_0} is slightly negative. Thermal expansion effects of the order of magnitude of that measured by Fritsch et al (ref 4) yield isobaric $\rho(T)$ which are in reasonable agreement with the forms observed in simple metal amorphous alloys. Note, in particular, the dramatic reductions in the size of the maximum in $\rho(T)$ and its movement to lower T_M as w varies from 0 to -0.5 .

Figure 4 shows results computed in the constant t -matrix approximation as described in Reference 16, at $2k_F = 1.15 k_p$ and $q_D\Lambda = 12$. The isochoric and negative w curves in this figure are not significantly different from those computed for the Mg and Zn phase shifts with $2k_F = 1.11 k_p$, and $q_D\Lambda = 17.1$

shown in Figure 2. This figure illustrates the reduction in magnitude and motion of the maximum in $\rho(T)$ as w varies from +0.2 to -0.5. For w values slightly more negative than -0.5, $\rho(T)$ is monotonic decreasing with increasing T and for $w = +0.5$, the maximum in $\rho(T)$ is gone and Γ is positive.

Figure 5 shows results in the constant t -matrix approximation (as in Figure 4) with $2k_F = 1.3 k_p$ and $q_D \Lambda = 6$. These curves are thus appropriate to larger electron per atom ratio z and resistivity than those shown in Figures 2 through 4. We would not consider a calculation for $q_D \Lambda = 6$ as representative of low ρ alloys. The isochoric $\rho(T)$ has a small negative Γ and a maximum near $\theta/4$, the positive w curves have positive Γ and no maxima, the curve for $w = -0.2$ has a small maximum near $\theta/6$ and negative Γ , and the curve for $w = -0.5$ is monotonic decreasing.

The curves shown in Figures 3 through 5 are not intended to provide an exhaustive survey of the possibilities for the inclusion of thermal expansion effects in $\rho(T)$ by any means. For example, each of the sixty isochoric results presented in Reference 16 could be the basis for a set of isobaric results for different $w(T)$. Thus, the present selection is necessarily somewhat arbitrary.

An interesting case, which we have not shown in the figures is ρ versus T for extreme saturation ($q_D \Lambda \rightarrow 1$). It is possible to select positive w values in this limit which yield ρ versus T curves which resemble those seen in very high resistivity ($\rho \geq 200 \mu\Omega\text{cm}$) metals (ref 20). However, the choice of parameters (α and w) to fit observed $\rho(T)$ seems to be too limited to explain an apparently universal form. Perhaps realistic T -dependent $w(T)$ could explain the extreme saturation $\rho(T)$ forms.

Another interesting case not illustrated is the moderate or low ρ alloy, whose isochoric $\rho(T)$ has $\Gamma_{V_0} > 0$. For such alloys (with positive Γ) inclusion of thermal expansion can yield the typically observed negative Γ with appropriate maximum, etc.

Let us now address the general question of thermal expansion effects in actual amorphous alloys. Let TM stand for a transition metal constituent, M stand for a non-TM metallic constituent, and NM a non-metallic constituent. Fritsch et al (ref 4) made the following observations concerning the pressure coefficient of resistivity Γ in amorphous alloys: (1) M-TM alloys exhibit negative Π ; (2) TM-TM alloys exhibit negative Π ; and (3) NM-TM systems exhibit negative or small Π . Essentially the same conclusions were drawn by Cote and Meisel (ref 2) (based on considerably less data) in their earlier study of pressure effects in electrical transport. However, in contrast to Cote and Meisel (ref 2), Fritsch, et al (ref 4) also concluded that there is no correlation between the Π and the magnitude of ρ . It appears to us that the data of Fritsch, et al (ref 4) are, in fact, consistent with our conclusion that the envelope of Π versus ρ values becomes narrower at higher ρ values, although the narrowing is not as rapid as estimated in Reference 2. Also, one should note that the higher ρ amorphous alloys tend to be less compressible than the low ρ alloys so that the narrowing of the envelope of the Π versus ρ data may be equivalent to a ρ independent envelope for $(\partial \ln \rho / \partial \ln V)_{T, V_0}$ versus ρ .

No general conclusions concerning Π in low ρ or M-M amorphous alloys can be drawn from extant pressure data. However, there are reasons to believe that Π may be positive or small for M-M amorphous alloys: (1) the only system

studied (a-Mg₇Zn₃) exhibits a relatively large positive Π ; (2) values of $q_D \Lambda$ smaller than those indicated by Eq. (11) and/or significantly smaller θ than the thermal values are required in the context of the diffraction model to yield isochoric $\rho(T, V_0)$ which are in agreement with the extensive body of isobaric $\rho(T)$ data in M-M amorphous alloys determined by Mizutani and coworkers (refs 7,21). The discrepancies between the observed isobaric $\rho(T)$ and the computed isochoric $\rho(T, V_0)$, without adjusted $q_D \Lambda$ and θ are consistent with a thermal expansion contribution appropriate for positive Π . (This picture appears to hold together in detail for a-Mg₇Zn₃.)

Thus, the curves in Figures 3 through 5 for $w \geq 0$ are representative of high ρ ($\rho > 100 \mu\Omega\text{cm}$) alloys, which are generally TM-TM, M-TM, or NM-TM systems; and the curves in Figures 2 through 5 for $w \leq 0$ are (tentatively) representative of low ρ ($\rho < 100 \mu\Omega\text{cm}$) alloys, which are generally M-M systems. We keep in mind that in general $w(T)$ will be T-dependent and allow for the possibility of T-dependent linear interpolation or extrapolation of these curves. The form of $F(T/\theta)$ shown in Figure 1 can, of course, be combined with arbitrary isochoric $\rho(T, V_0)$ (or $R(T, V_0)/\alpha$) and appropriate $K(T)$ (or $w(T)$) to obtain isobaric $\rho(T)$ (or $r(T)$) curves.

CONCLUSIONS

1. Thermal expansion effects are important in determining isobaric $\rho(T)$ in amorphous metals. Such effects are independent of the particular treatment appropriate to the isochoric problem. For example, thermal expansion contributes at least 25 percent of the observed isobaric temperature coefficient of resistivity Γ in a-Mg₇Zn₃.

2. All TM-TM, M-TM, and NM-T, amorphous alloys studied (which generally have $\rho > 100 \mu\Omega\text{cm}$) have small or negative pressure coefficient of resistivity Π and hence, from Eq. (13), have small or positive $w(T)$.

Values of Π are not available for M-M and/or low resistivity amorphous metals, with the notable exception of a-Mg₇Zn₃. However, the preponderance of relatively large negative isobaric Γ values in the alloys studied (refs 7,21) and the observation in a-Mg₇Zn₃ suggests that positive or small Π , and hence negative or small $w(T)$, may be appropriate for these low resistivity alloys.

3. Alloys having negative Γ exhibit either monotonic decreasing $\rho(T)$ or a maximum in $\rho(T)$. The $\rho(T)$ exhibiting a maximum often exhibit a minimum in $\rho(T)$ at a lower T as well. In some of the cases where a minimum is not observed, the possibility of the observation of a minimum is precluded by lack of experimental precision or a transition to the superconducting state.

Monotonic decreasing $\rho(T)$ is usually observed in high ρ cases (refs 9,20) and the maximum (with or without minimum) in $\rho(T)$ is usually observed in low ρ or moderate ρ cases. (We suggest that these forms for $\rho(T)$ result from Pippard-Ziman saturation (refs 9,11-13) with appropriate $q_D \Lambda$.)

The effect of thermal expansion on $\rho(T)$ having a maximum for positive (negative) $w(T)$ is to increase (decrease) the size of the maximum and to move the maximum to higher (lower) temperature than given by isochoric theory. It is also possible for thermal expansion with positive $w(T)$ to produce isobaric $\rho(T)$ with minimum and maximum for monotonic decreasing isochoric $\rho(T, V_0)$ and vice versa. (Note that thermal expansion described by Gruneisen theory, i.e., Eqs. (3) and (4), has negligible effect at the temperatures where minima have been observed.)

Thermal expansion effects with positive $w(T)$ can produce upward curvature for $T \geq \theta/5$ in monotonic decreasing $\rho(T)$ curves. Such curvature is observed in some high ρ alloys.

4. Positive Γ alloys are predominantly of low resistivity ($\rho \lesssim 100 \mu\Omega\text{cm}$) and one can expect to find upward (downward) curvature in $\rho(T)$ for $T \geq \theta/5$ for $w(T)$ positive (negative). We have also shown that thermal expansion effects for positive $w(T)$ can yield isobaric $\rho(T)$ with positive Γ for isochoric $\rho(T, V_0)$ having maximum, minimum, and negative Γ_{V_0} and vice versa.

5. Thermal expansion effects are important in determining $\rho(T)$ in the specific case of $a\text{-Mg}_7\text{Zn}_3$. Good agreement with the data is obtained with Gruneisen thermal expansion theory, Eqs. (3) and (4), with $w(T)$ assumed constant equal to $w(\theta)$ empirical or thermal values of parameters and diffraction model transport incorporating Pippard-Ziman saturation with $q_D \Lambda = 17.1$ and scattering phase shifts based on Herman-Skillman neutral atom wavefunctions (ref 15). Hafner (ref 5) also obtained good agreement with the $a\text{-Mg}_7\text{Zn}_3$ resistivity data in a first principles pseudopotential based standard (i.e., no saturation) diffraction model calculation which incorporated thermal expansion effects.

Besides serving to demonstrate the importance of thermal expansion effects in electrical transport in amorphous metals, the $a\text{-Mg}_7\text{Zn}_3$ results raise some disturbing questions concerning diffraction model procedures. For example, the low temperature minimum in $\rho(T)$, which in our calculations is a saturation effect, is a consequence of some feature of the standard diffraction model in Hafner's work. We do not know which features of Hafner's work are significantly different from ours. Is Hafner's self-consistent

phonon spectrum significantly different from the Debye form? Is his treatment of thermal expansion significantly different from the simple Gruneisen approach adopted here? These (and other) questions are presently unresolved.

REFERENCES

1. D. Lazarus, *Solid State Commun.* 32, 175 (1979); R. W. Cochrane, J. O. Strom-Olsen, J. P. Rebouillat, and A. Blanchard, *Solid State Commun.* 35, 199 (1980); D. G. Ast and D. J. Krenitsky, *Scr. Metall.* 10, 247 (1976).
2. P. J. Cote and L. V. Meisel, *Phys. Rev.* 25, 2138 (1982).
3. See, for example, P. W. Bridgman, *The Physics of High Pressure* (Bell, London, 1949).
4. G. Fritsch, J. Willer, A. Wildermuth, and E. Luscher, *J. Phys. F.* 12, 2965 (1982); E. Luscher, J. Willer, G. Fritsch, *J. Non-Cryst Solids* 62, 1109 (1984).
5. J. Hafner, *J. Non-Cryst. Solids*, to be published.
6. See, for example, J. M. Ziman, *Electrons and Phonons* (Clarendon, Oxford, 1960), pp. 152-156. A recent review of Gruneisen theory may be found in T. H. K. Barron, J. G. Collins, and G. K. White, "Advances in Physics," 26, 609 (1980).
7. T. Matsuda and U. Mizutani, *J. Phys. F* 12, 1877 (1982); U. Mizutani and T. Mizoguchi, *J. Phys. F.* 11, 1385 (1981); T. Mizoguchi, N. Shiotani, U. Mizutani, T. Kudo, and S. Yamada, *J. Phys. (Paris) Colloq.* 41 C8-183 (1980).
8. G. Baym, *Phys. Rev.* 135, A1691 (1964); L. van Hove, *Phys. Rev.* 95, 294 (1954); T. E. Faber and J. M. Ziman, *Phil. Mag.* 11, 153 (1965); P. J. Cote and L. V. Meisel, *Phys. Rev. Lett.* 39, 102 (1977); L. V. Meisel and P. J. Cote, *Phys. Rev.* 16, 2978 (1977); K. Frobose and J. Jackle, *J. Phys. F* 1, 2331 (1977).

9. See, for example, P. J. Cote and L. V. Meisel in Glassy Metals I, edited by H. J. Guntherodt and H. Beck (Springer, Heidelberg, 1981).
10. L. V. Meisel and P. J. Cote, Phys. Rev. B 27, 4617 (1983).
11. P. J. Cote and L. V. Meisel, Phys. Rev. Lett. 40, 1586 (1978).
12. A. Schmidt, Z. Phys. 259, 421 (1973).
13. See Reference 6, Ch. V.
14. P. J. Cote and L. V. Meisel, J. Non-Cryst. Solids 62, 1167 (1984).
15. F. C. Herman and S. Skillman, Atomic Structure Calculations, (Prentice Hall, Englewood Cliffs, NJ, 1963).
16. L. V. Meisel and P. J. Cote, Phys. Rev., to be published.
17. K. A. Gschneidner, Solid State Physics, Vol. 16, edited by F. Seitz and D. Turnbull (Academic, New York, 1964).
18. W. A. Harrison, Pseudopotentials in the Theory of Metals, (Benjamin, New York, 1966).
19. W. H. Young, Axel Meyer, and G. E. Kilby, Phys. Rev. 160 (1967).
20. See, for example, J. H. Mooij, Phys. Status Solidi (a) 17, 521 (1972); and Reference 9 (and references therein).
21. For example, U. Mizutani and T. Yoshina, J. Phys. F 12, 2331 (1982); T. Matsuda and U. Mizutani, Solid State Commun. 44, 145 (1982); T. Matsuda, N. Shiotani, and U. Mizutani, J. Phys. F 14, 1193 (1984); U. Mizutani and T. Matsuda, J. Phys. F (to be published).

TABLE I. PARAMETERS EMPLOYED IN THE α -Mg₇Zn₃ CALCULATIONS

$\theta = 295\text{K}$ is from Mizutani and Mizoguchi in Reference 7.

$2k_F/k_P = 1.11$ where k_F is from Matsuda and Mizutani in Reference 7.

and k_P is from Mizoguchi et al in Reference 7.

$\rho_D = k_F$ and single branch Debye spectrum are assumed.

Values at 300K	Gschneider ¹⁷			Fritsch et al ⁴ a-Mg ₇ Zn ₃	Hafner ⁵ a-Mg ₇ Zn ₃
	Mg	Zn	a-Mg ₇ Zn ₃ *		
B_T (kbar)	361	610	436	400	509
$10^6 \beta_V$ (K ⁻¹)	76.8	89.1	80.5		59
γ	1.63	2.05	1.76		
V_0 (cm ³ /gmAt)	14.00	9.17	12.6		
$10^3 \Pi$ (kbar ⁻¹)				2.39	4.8

*These values, which are computed by the "law of mixtures", and the pressure coefficient of resistivity Π values shown are used in the transport calculations.

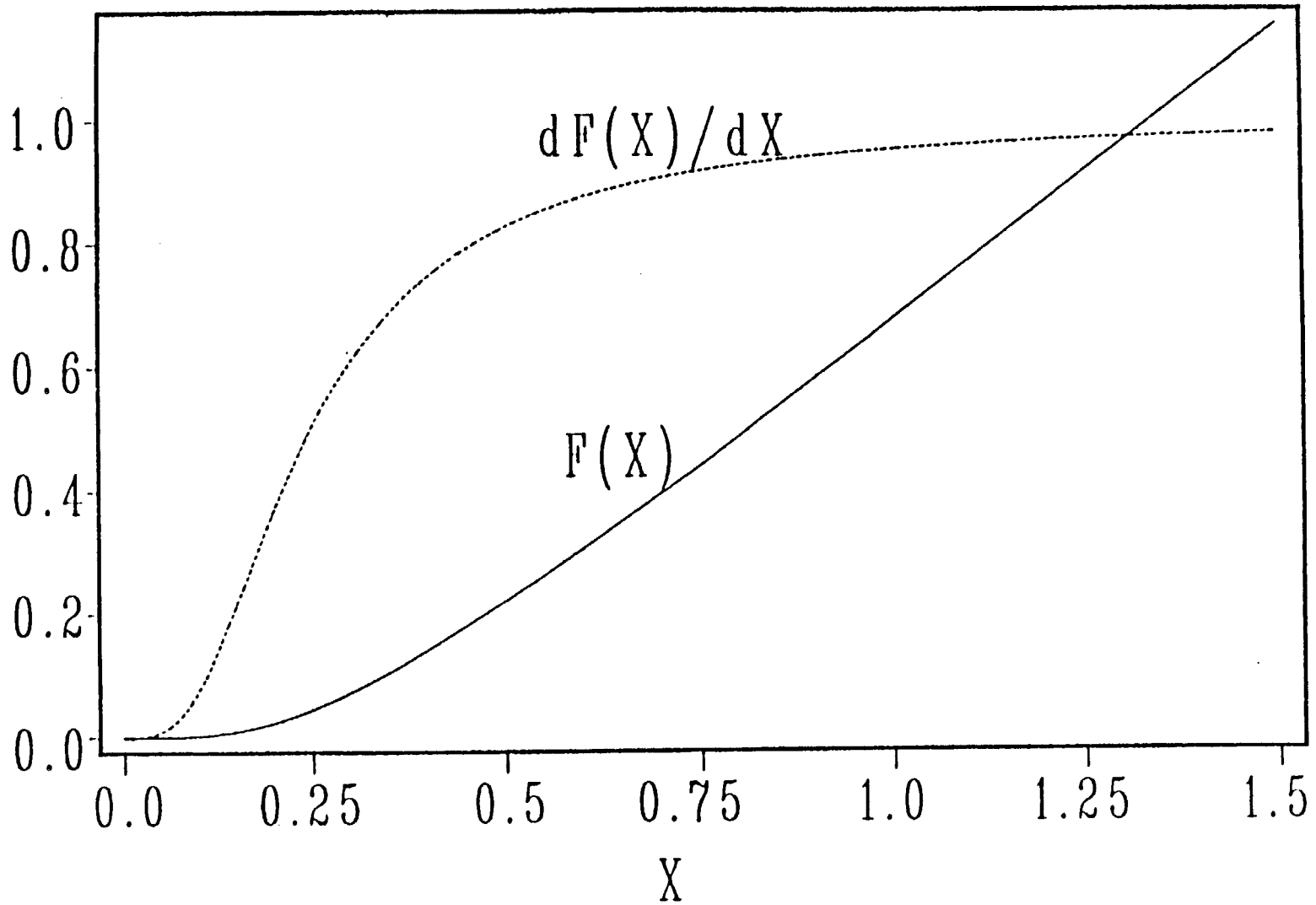


Figure 1. The Gruneisen integral, defined in Eq. (4b), and its first derivative.

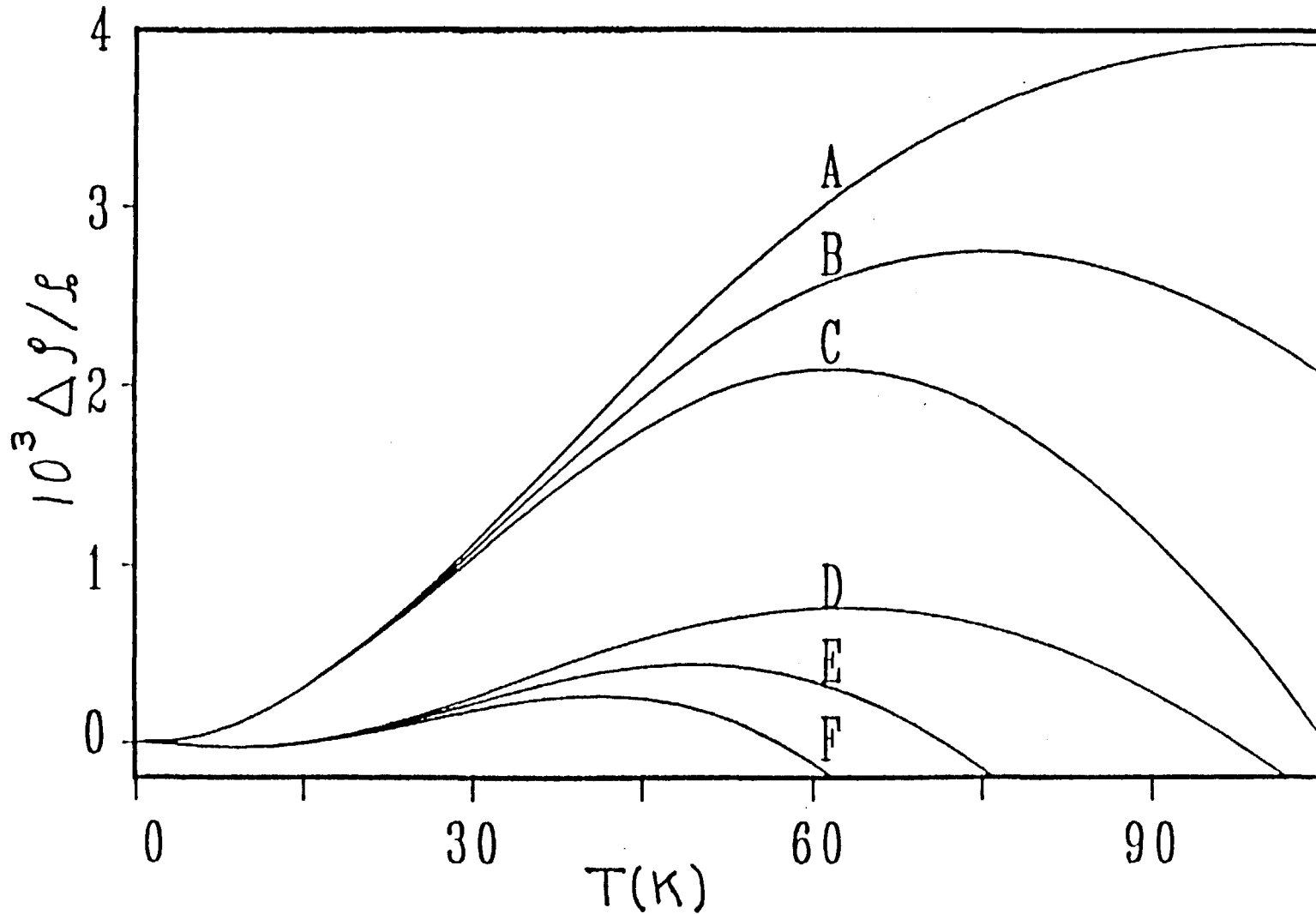


Figure 2. The relative change in resistivity versus temperature for α - Mg_7Zn_3 based on the parameters in Table I. Curves A, B, and C are computed for $q_D\Lambda = \infty$ (the standard diffraction model); curves D, E, F for $q_D\Lambda = 17.1$. Curves A and D are isochores. Curves B and E include thermal expansion effects with the measured (ref 4) C_{PCR} . Curves C and F include thermal expansion effects with Hafner's (ref 5) theoretical C_{PCR} .

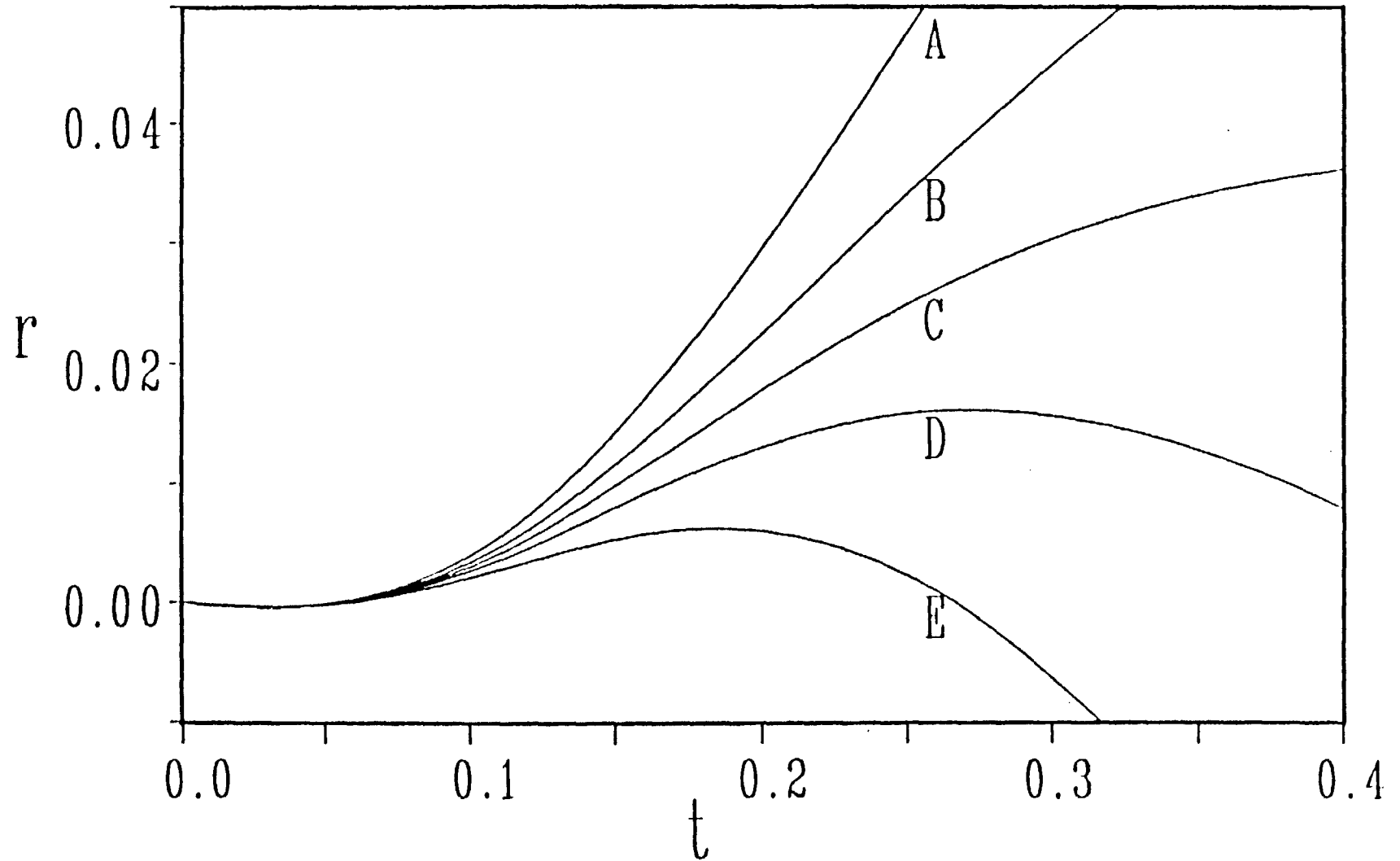


Figure 3. Normalized resistivity difference versus normalized temperature for potassium pseudoatom phase shifts (ref 19) with $2k_F/k_p = 1.1$ and $q_D\Lambda = 12$. The p values are 0.5, 0.2, 0, -0.2, and -0.5 for curves A, B, C, D, and E, respectively.

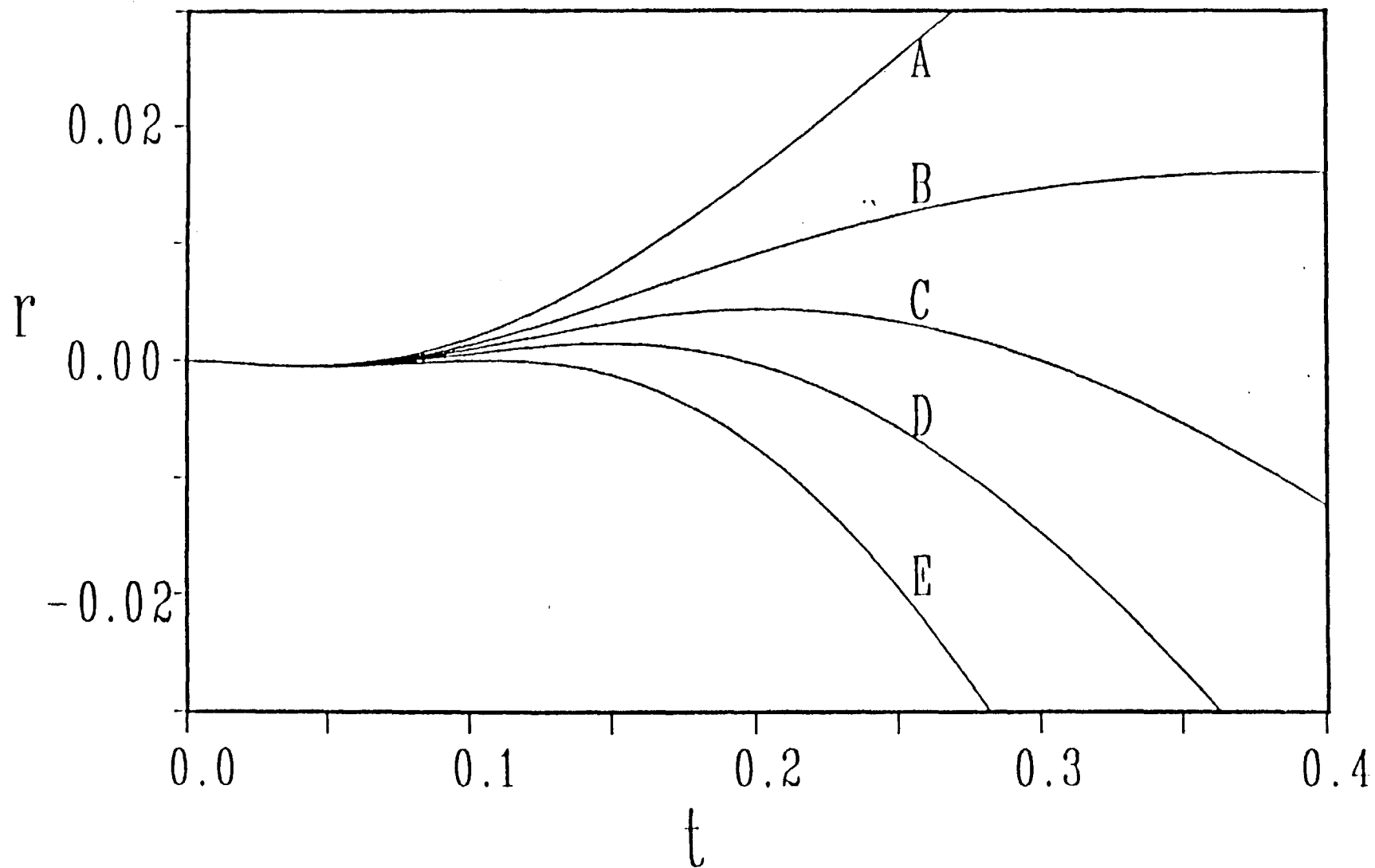


Figure 4. Results computed in the constant t-matrix effective potential approximation (ref 16) with $2k_F/k_p = 1.15$ and $q_D\Lambda = 12$.

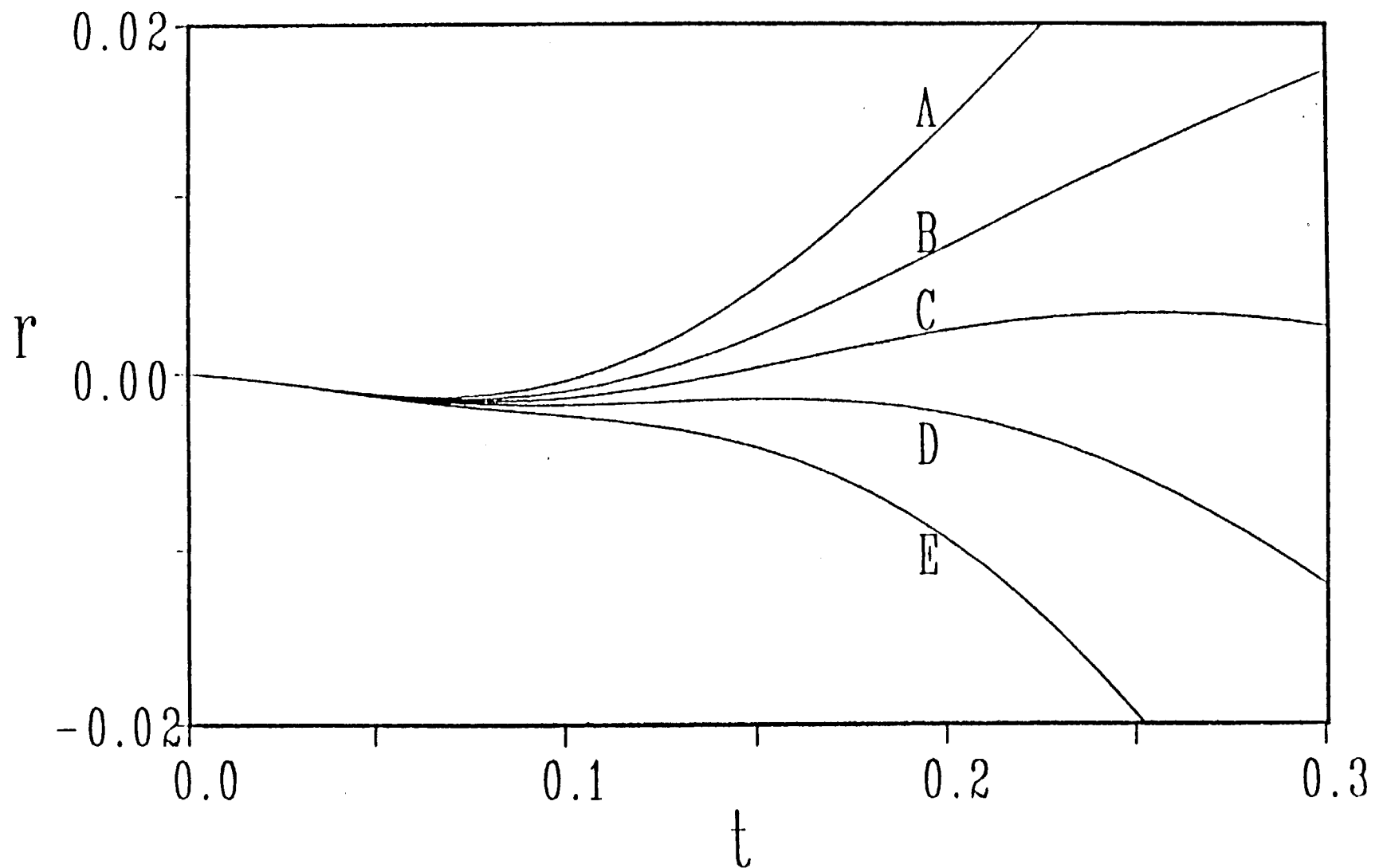


Figure 5. Results computed in the constant t-matrix effective potential approximation (ref 16) with $2k_F/k_p = 1.30$ and $q_D\Lambda = 6$.

TECHNICAL REPORT INTERNAL DISTRIBUTION LIST

	<u>NO. OF COPIES</u>
CHIEF, DEVELOPMENT ENGINEERING BRANCH	
ATTN: SMCAR-LCB-D	1
-DA	1
-DP	1
-DR	1
-DS (SYSTEMS)	1
-DS (ICAS GROUP)	1
-DC	1
CHIEF, ENGINEERING SUPPORT BRANCH	
ATTN: SMCAR-LCB-S	1
-SE	1
CHIEF, RESEARCH BRANCH	
ATTN: SMCAR-LCB-R	2
-R (ELLEN FOGARTY)	1
-RA	1
-RM	2
-RP	1
-RT	1
TECHNICAL LIBRARY	5
ATTN: SMCAR-LCB-TL	
TECHNICAL PUBLICATIONS & EDITING UNIT	2
ATTN: SMCAR-LCB-TL	
DIRECTOR, OPERATIONS DIRECTORATE	1
DIRECTOR, PROCUREMENT DIRECTORATE	1
DIRECTOR, PRODUCT ASSURANCE DIRECTORATE	1

NOTE: PLEASE NOTIFY DIRECTOR, BENET WEAPONS LABORATORY, ATTN: SMCAR-LCB-TL,
OF ANY ADDRESS CHANGES.

TECHNICAL REPORT EXTERNAL DISTRIBUTION LIST

	<u>NO. OF COPIES</u>		<u>NO. OF COPIES</u>
ASST SEC OF THE ARMY RESEARCH & DEVELOPMENT ATTN: DEP FOR SCI & TECH THE PENTAGON WASHINGTON, D.C. 20315	1	COMMANDER US ARMY AMCCOM ATTN: SMCAR-ESP-L ROCK ISLAND, IL 61299	1
COMMANDER DEFENSE TECHNICAL INFO CENTER ATTN: DTIC-DDA CAMERON STATION ALEXANDRIA, VA 22314	12	COMMANDER ROCK ISLAND ARSENAL ATTN: SMCRI-ENM (MAT SCI DIV) ROCK ISLAND, IL 61299	1
COMMANDER US ARMY MAT DEV & READ COMD ATTN: DRCDE-SG 5001 EISENHOWER AVE ALEXANDRIA, VA 22333	1	DIRECTOR US ARMY INDUSTRIAL BASE ENG ACTV ATTN: DRXIB-M ROCK ISLAND, IL 61299	1
COMMANDER ARMAMENT RES & DEV CTR US ARMY AMCCOM ATTN: SMCAR-LC SMCAR-LCE SMCAR-LCM (BLDG 321) SMCAR-LCS SMCAR-LCU SMCAR-LCW SMCAR-SCM-O (PLASTICS TECH EVAL CTR, BLDG. 351N) SMCAR-TSS (STINFO) DOVER, NJ 07801	1 1 1 1 1 1 1 2	COMMANDER US ARMY TANK-AUTMV R&D COMD ATTN: TECH LIB - DRSTA-TSL WARREN, MI 48090	1
		COMMANDER US ARMY TANK-AUTMV COMD ATTN: DRSTA-RC WARREN, MI 48090	1
		COMMANDER US MILITARY ACADEMY ATTN: CHMN, MECH ENGR DEPT WEST POINT, NY 10996	1
DIRECTOR BALLISTICS RESEARCH LABORATORY ATTN: AMXBR-TSB-S (STINFO) ABERDEEN PROVING GROUND, MD 21005	1	US ARMY MISSILE COMD REDSTONE SCIENTIFIC INFO CTR ATTN: DOCUMENTS SECT, BLDG. 4484 REDSTONE ARSENAL, AL 35898	2
MATERIEL SYSTEMS ANALYSIS ACTV ATTN: DRXSY-MP ABERDEEN PROVING GROUND, MD 21005	1	COMMANDER US ARMY FGN SCIENCE & TECH CTR ATTN: DRXST-SD 220 7TH STREET, N.E. CHARLOTTESVILLE, VA 22901	1

NOTE: PLEASE NOTIFY COMMANDER, ARMAMENT RESEARCH AND DEVELOPMENT CENTER,
US ARMY AMCCOM, ATTN: BENET WEAPONS LABORATORY, SMCAR-LCB-TL,
WATERVLIET, NY 12189, OF ANY ADDRESS CHANGES.

TECHNICAL REPORT EXTERNAL DISTRIBUTION LIST (CONT'D)

	<u>NO. OF COPIES</u>		<u>NO. OF COPIES</u>
COMMANDER US ARMY MATERIALS & MECHANICS RESEARCH CENTER ATTN: TECH LIB - DRXMR-PL WATERTOWN, MA 01272	2	DIRECTOR US NAVAL RESEARCH LAB ATTN: DIR, MECH DIV CODE 26-27, (DOC LIB) WASHINGTON, D.C. 20375	1 1
COMMANDER US ARMY RESEARCH OFFICE ATTN: CHIEF, IPO P.O. BOX 12211 RESEARCH TRIANGLE PARK, NC 27709	1	COMMANDER AIR FORCE ARMAMENT LABORATORY ATTN: AFATL/DLJ AFATL/DLJG EGLIN AFB, FL 32542	1 1
COMMANDER US ARMY HARRY DIAMOND LAB ATTN: TECH LIB 2800 POWDER MILL ROAD ADELPHIA, MD 20783	1	METALS & CERAMICS INFO CTR BATTELLE COLUMBUS LAB 505 KING AVENUE COLUMBUS, OH 43201	1
COMMANDER NAVAL SURFACE WEAPONS CTR ATTN: TECHNICAL LIBRARY CODE X212 DAHLGREN, VA 22448	1		

NOTE: PLEASE NOTIFY COMMANDER, ARMAMENT RESEARCH AND DEVELOPMENT CENTER,
US ARMY AMCCOM, ATTN: BENET WEAPONS LABORATORY, SMCAR-LCB-TL,
WATERVLIET, NY 12189, OF ANY ADDRESS CHANGES.